

Density Functional Theory Investigations of the Homoleptic Tris(dithiolene) Complexes $[M(\text{ddd}t)_3]^{-q}$ ($q = 3, 2$; $M = \text{Nd}^{3+}$ and $\text{U}^{3+/4+}$) Related to Lanthanide(III)/Actinide(III) Differentiation

Samir Meskaldji,[†] Lotfi Belkhiri,[†] Thérèse Arliguie,[‡] Marc Fourmigué,^{||} Michel Ephritikhine,[‡] and Abdou Boucekkine^{*,||}

[†]Unité de Recherche Chimie de l'Environnement et Moléculaire Structurale (URCHEMS), Université Mentouri de Constantine, 25017 Constantine, Algeria, [‡]CEA, IRAMIS, SIS2M, CNRS UMR 3299, CEA/Saclay, 91191 Gif-sur-Yvette, France, and ^{||}UMR CNRS 6226 Sciences Chimiques de Rennes, Université de Rennes 1, Campus de Beaulieu, 35042 Rennes Cedex, France

Received October 27, 2009

The structures of the homoleptic lanthanide and actinide tris(dithiolene) complexes $[M(\text{ddd}t)_3]^{q-}$ ($q = 3, M = \text{Nd}^{3+}$ and $q = 3$ or $2, M = \text{U}^{3+/4+}$) have been investigated using relativistic Density Functional Theory (DFT) computations including spin–orbit corrections coupled with the COnductor–like Screening Model (COSMO) for a realistic solvation approach. The dithiolene ligands are known to be very efficient at stabilizing metal high oxidation states. The aim of the work is to explain the peculiar symmetric folding of the three Mddd metallacycles in these complexes, some of them existing under a polymeric form, in relation with the Ln(III)/An(III) differentiation. In the $[M(\text{ddd}t)_3(\text{py})]^{q-}$ species, where an additional pyridine ligand is linked to the metal center, the Mddd moieties appear to be almost planar. The study brings to light the occurrence of a $M \cdots C=C$ interaction explaining the Mddd folding of the $[\text{U}(\text{ddd}t)_3]^{q-}$ uranium species, the metal 5f electrons playing a driving role. No such interaction appears in the case of the Nd(III) complex, and the folding of the rather flexible dddt ligands in the polymeric structure of this species should be mainly due to steric effects. Moreover, the analysis of the normal modes of vibration shows that the U(III) complex $[\text{U}(\text{ddd}t)_3]^{3-}$, which has not yet been isolated, is thermodynamically stable. It appears that the X-ray characterized U(IV) complex $[\text{U}(\text{ddd}t)_3]^{2-}$ should be less stable than the calculated U(III) complex in a polar solvent.

Introduction

The description of the electronic and molecular structures of f-element compounds is essential for the understanding of their chemical and physical properties and for the development of applications in many fields, from biology and medicine to materials science technology.¹ In the domain of the nuclear industry, the mechanisms of selective complexation of trivalent actinide An(III) and lanthanide Ln(III) ions attract much attention for their importance in the partitioning of spent nuclear fuels.^{2–6}

Although the degree of covalency in f-element compounds is still a matter of recurrent debate, it is established that metal–ligand bonding in Ln(III) complexes is of a stronger ionic character than in their An(III) analogues.^{7–10} Covalency

*To whom correspondence should be addressed. E-mail: abdou.boucekkine@univ-rennes1.fr.

(1) (a) *The Chemistry of the Actinide and Transactinide Elements*, 3rd ed.; Morss, L. R., Edelstein, N., Fuger, J., Katz, J. J., Eds.; Springer: Dordrecht, The Netherlands, 2006. (b) Ephritikhine, M. *Dalton Trans.* 2006, 2501.

(2) Arliguie, T.; Belkhiri, L.; Bouaoud, S. E.; Thuéry, P.; Villiers, C.; Boucekkine, A.; Ephritikhine, M. *Inorg. Chem.* 2009, 48, 221.

(3) Mehdoui, T.; Berthet, J. C.; Thuéry, P.; Ephritikhine, M. *Chem. Commun.* 2005, 2860.

(4) Berthet, J. C.; Nierlich, M.; Miquel, Y.; Madic, C.; Ephritikhine, M. *Dalton Trans.* 2005, 369.

(5) Mehdoui, T.; Berthet, J. C.; Thuéry, P. *Dalton Trans.* 2005, 1263.

(6) Mehdoui, T.; Berthet, J. C.; Thuéry, P.; Salmon, L.; Rivière, E.; Ephritikhine, M. *Chem.—Eur. J.* 2005, 11, 6994.

(7) (a) Sockwell, S. C.; Hanusa, T. P. *Inorg. Chem.* 1990, 29, 76. (b) Vetere, V.; Maldivi, P.; Adamo, C. *J. Comput. Chem.* 2003, 24, 850. (c) Guillaumont, D. *J. Phys. Chem. A* 2004, 108, 6893. (d) Petit, L.; Joubert, L.; Maldivi, P.; Adamo, C. *J. Am. Chem. Soc.* 2006, 128, 2190.

(8) (a) Boussie, T. R.; Eisenberg, D. C.; Rigsbee, J.; Streitwieser, A.; Zalkin, A. *Organometallics* 1991, 10(1991), 1922. (b) Dolg, M.; Fulde, P. *Chem.—Eur. J.* 1998, 4, 200. (c) Choppin, G. R. *J. Alloys Cpd.* 2002, 344, 55. (d) Sabirov, Z. M.; Bagatur'yants, A. A. *Russ. Chem. Rev.* 1991, 60, 1059.

(9) (a) Bursten, B. E.; Casarin, M.; Di Bella, S.; Fang, A.; Fraga, I. L. *Inorg. Chem.* 1985, 24, 2169. (b) Bursten, B. E.; Rhodes, L. F.; Strittmatter, R. J. *J. Am. Chem. Soc.* 1989, 111, 2756. (c) Strittmatter, R. J.; Bursten, B. E. *J. Am. Chem. Soc.* 1991, 113, 552. (d) Bursten, B. E.; Strittmatter, R. J. *Angew. Chem., Int. Ed. Engl.* 1991, 30, 1069. (e) Kaltsoyannis, N.; Bursten, B. E. *J. Organomet. Chem.* 1997, 528, 19. (f) Schreckenbach, G.; Jeffrey, P. H.; Richard, L. M. *J. Comput. Chem.* 1999, 20, 7090. (g) Kaltsoyannis, N.; Scott, P. *The f Elements*; Oxford Chemistry Publications Eds: Oxford, U. K., 1999; p 10. (h) Cloke, F. G. N.; Green, J. C.; Kaltsoyannis, N. *Organometallics* 2004, 23, 832.

(10) (a) Arliguie, T.; Fourmigué, M.; Ephritikhine, M. *Organometallics* 2000, 19, 109. (b) Belkhiri, L.; Arliguie, T.; Thuéry, P.; Fourmigué, M.; Boucekkine, A.; Ephritikhine, M. *Organometallics* 2006, 25, 2782. (c) Roger, M.; Belkhiri, L.; Thuéry, P.; Arliguie, T.; Fourmigué, M.; Boucekkine, A.; Ephritikhine, M. *Organometallics* 2005, 24, 4940.

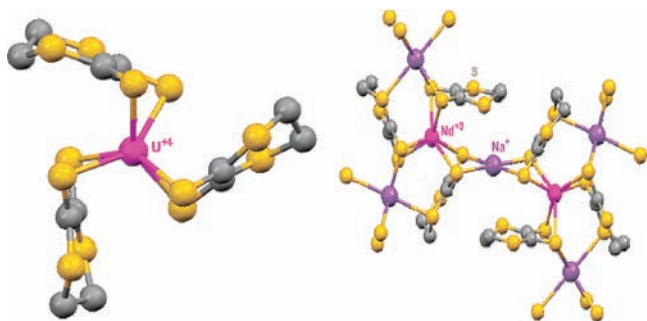


Figure 1. Views of the U(IV) $[U(dddt)_3]^{2-}$ ion and of a fragment of the anionic Nd(III) $[Na_{1.5}Nd(dddt)_3]^{1.5-}$ polymer. H atoms have been omitted for clarity.

(the mixing of orbitals) in metal–ligand bonding is expected to play a key role in Ln(III)/An(III) differentiation. Furthermore, the spectroscopy, reactivity, and structural chemistry of actinides compounds suggest that the 5f electrons are far more involved in chemical bonding than previously thought.¹¹

The dddt dithiolene ligand (dddt = 5,6-dihydro-1,4-dithiine-2,3-dithiolate) has been used in lanthanide and actinide chemistry as well as in d transition metal chemistry to stabilize electronically unsaturated metal centers.¹² This is due to the combination of its steric encumbrance and the availability of “big” lone pairs on the sulfur donor atoms.

In this context, we found it interesting to computationally investigate our recently reported homoleptic tris(dithiolene) $M(dddt)_3$ complexes of lanthanides and uranium.¹³ The lanthanide compounds were structurally characterized as the mononuclear ion $[Nd(dddt)_3(py)]^{3-}$ and the polymeric 1D chains or 2D layers where the $[Nd(dddt)_3]$ or $[Ln(dddt)_3(py)]$ fragments ($Ln = Ce, Nd$) are bridged by Na atoms or $M_2(18\text{-crown-6})$ moieties ($M = Na, K$). Homoleptic uranium dithiolene complexes were isolated in the +4 oxidation state as the mononuclear tris(dithiolene) $[U(dddt)_3]^{2-}$ ion and the infinite chains in which the tetrakis(dithiolene) unit $[U(dddt)_4]$ is surrounded by four Na atoms, two of those being involved in bridging $Na_2(\mu\text{-THF})_3$ fragments.^{13a} The synthesis of the U(III) species $[U(dddt)_3]^{3-}$ has been so far unsuccessful.^{13b} It is noteworthy that the $[Nd(dddt)_3]$ moieties in the polymeric anion $[Na_{1.5}Nd(dddt)_3]^{1.5-}$ exhibit a very large folding of the MS_2C_2 metallacycle (around 80°), as large as the one observed in the mononuclear uranium(IV) $[U(dddt)_3]^{2-}$ ion (Figure 1).

(11) (a) Morris, D. E.; Da Re, R. E.; Jantunen, K. C.; Castro-Rodriguez, I.; Kiplinger, J. L. *Organometallics* **2004**, *23*, 5142. (b) Belkhir, L.; Lissillour, R.; Boucekkine, A. *J. Mol. Struct. (THEOCHEM)* **2005**, *757*, 155. (c) Shamov, G. A.; Schreckenbach, G. *J. Phys. Chem. A* **2005**, *109*, 10961. (d) BenYahia, M.; Belkhir, L.; Boucekkine, A. *J. Mol. Struct. (THEOCHEM)* **2006**, *777*, 61. (e) Schelter, E. J.; Yang, P.; Scott, B. L.; Thompson, J. D.; Martin, R. L.; Hay, P. J.; Morris, D. E.; Kiplinger, J. L. *Inorg. Chem.* **2007**, *46*, 7477. (f) Gaunt, A. J.; Reilly, S. D.; Enriquez, A. E.; Scott, B. L.; Ibers, J. A.; Sekar, P.; Ingram, K. I. M.; Kaltsyannis, N.; Neu, M. P. *Inorg. Chem.* **2008**, *47*, 29. (g) Graves, C. R.; Yang, P.; Kozimor, S. A.; Vaughn, A. E.; Clark, D. L.; Conradson, S. D.; E. Schelter, E. J.; Scott, B. L.; Thompson, J. D.; Hay, P. J.; Morris, D. E.; Kiplinger, J. L. *J. Am. Chem. Soc.* **2008**, *130*, 5272. (h) Gaunt, A. J.; Reilly, S. D.; Enriquez, A. E.; Scott, B. J.; Ibers, J. A.; Sekar, P.; Ingram, K. I. M.; Kaltsyannis, N.; Neu, M. P. *Inorg. Chem.* **2008**, *47*, 29.

(12) (a) Arliguie, T.; Fourmigué, M.; Ephritikhine, M. *Organometallics* **2000**, *19*, 109. (b) Domercq, B.; Coulon, C.; Fourmigué, M. *Inorg. Chem.* **2001**, *40*, 371. (c) Arliguie, T.; Thuéry, P.; Fourmigué, M.; Ephritikhine, M. *Organometallics* **2003**, *22*, 3000. (d) Arliguie, T.; Thuéry, P.; Leverd, P. C.; Fourmigué, M.; Ephritikhine, M. *Eur. J. Inorg. Chem.* **2004**, 4502.

(13) (a) Roger, M.; Arliguie, T.; Thuéry, P.; Fourmigué, M.; Ephritikhine, M. *Inorg. Chem.* **2005**, *44*, 584. (b) Roger, M.; Arliguie, T.; Thuéry, P.; Fourmigué, M.; Ephritikhine, M. *Inorg. Chem.* **2005**, *44*, 594.

As a consequence, the C=C double bond of the dithiolene ligand is close to the central metal with a $M \cdots (C=C)$ distance comparable to the $U-C(Cp^*)$ “long organometallic distances” observed in tris(pentamethylcyclopentadienyl) U(IV) complexes (2.780–2.920 Å).¹⁴

Particularly short $U \cdots (C=C)$ distances, from 2.879(5) to 2.969(11) Å, were measured in the crystal structures of a series of neutral organometallic mono(cyclooctatetraenyl) dithiolene uranium complexes of general formula $[U(COT)(dithiolene)L_n]$ ($L =$ Lewis base)¹⁵ and in the monocyclooctatetraenyl U(V) derivative $[U(COT)(dddt)_2]^-$ ($COT = \eta^8\text{-C}_8\text{H}_8$),^{10a} where the occurrence of a $U(V) \cdots (C=C)$ interaction was confirmed by DFT calculations.^{10b} Such interaction is generally attributed to the big size of the 5f element and its great affinity toward the neighboring electronic density of an unsaturated bond.^{9c,d}

In view of these structural features, the aim of this work was to explain the extremely strong folding ($\approx 80^\circ$) of the $Mdddt$ metallacycle in the homoleptic uranium and rare-earth dithiolene complexes. Indeed, a more limited chelate fold of the dithiolene ligand ($< 50^\circ$) has been encountered many times in d-block coordination complexes, as for example in tris(dithiolene) of V,¹⁶ Mo,^{17,18} and Re,¹⁹ where it has been ascribed to a second-order Jahn–Teller effect.²⁰ From the high-symmetry trigonal-prismatic D_{3h} geometry, folding of the ligands lowers the symmetry to C_{3h} symmetry where an occupied (or partially occupied) ligand-centered orbital can thus mix with an empty d_{z^2} orbital. Depending on the metal and the oxidation state, this folding ranges between 0 and 30° . Similarly, many oxo-²¹ or Cp-bis(dithiolene) complexes²² of V, Cr, Mo, W, and Cp-monodithiolene

(14) (a) Evans, W. J.; Forrestal, K. J.; Ziller, J. W. *Angew. Chem., Int. Ed. Engl.* **1997**, *36*, 774. (b) Evans, W. J.; Kozimor, S. A.; Nyce, G. W.; Ziller, J. W. *J. Am. Chem. Soc.* **2003**, *125*, 13831. (c) Evans, W. J.; Kozimor, S. A.; Ziller, J. W. *J. Am. Chem. Soc.* **2003**, *125*, 14264. (d) Evans, W. J.; Kozimor, S. A.; Ziller, J. W.; Kaltsyannis, N. *J. Am. Chem. Soc.* **2004**, *126*, 14533. (e) Evans, W. J.; Kozimor, S. A.; Ziller, J. W. *Polyhedron* **2004**, *23*, 2689. (f) Evans, W. J.; Kozimor, S. A.; Ziller, J. W. *Organometallics* **2005**, *24*, 3407. (g) Evans, W. J.; Kozimor, S. A.; Ziller, J. W. *Chem. Commun.* **2005**, 4681.

(15) (a) Arliguie, T.; Thuéry, P.; Fourmigué, M.; Ephritikhine, M. *Organometallics* **2003**, *22*, 3000. (b) Arliguie, T.; Thuéry, P.; Fourmigué, M.; Ephritikhine, M. *Eur. J. Inorg. Chem.* **2004**, 4502. (c) Fourmigué, M.; Lenoir, C.; Coulon, C.; Guyon, F.; Amaudrut J. *Inorg. Chem.* **1995**, *34*, 4979.

(16) (a) Livage, C.; Fourmigué, M.; Batail, P.; Canadell, E.; Coulon, C. *Bull. Soc. Chim. Fr.* **1993**, *130*, 761. (b) Broderick, W. E.; McGhee, E. M.; Godfrey, M. R.; Hoffman, B. M.; Ibers, J. A. *Inorg. Chem.* **1989**, *28*, 2902. (c) Welch, J. H.; Bereman, R. D.; Singh, P. *Inorg. Chem.* **1988**, *27*, 2862. (d) Chung, G.; Bereman, R.; Singh, P. *J. Coord. Chem.* **1994**, *33*, 331.

(17) (a) Friedle, S.; Partyka, D. V.; Bennett, M. V.; Holm, R. H. *Inorg. Chim. Acta* **2006**, *359*, 1427. (b) Smith, A. E.; Schrauzer, G. N.; Mayweg, V. P.; Heinrich, W. *J. Am. Chem. Soc.* **1965**, *87*, 5798. (c) Wang, K.; McConnachie, J. M.; Stiefel, E. I. *Inorg. Chem.* **1999**, *38*, 4334. (d) Cowie, M.; Bennett, M. J. *Inorg. Chem.* **1975**, *15*, 1584.

(18) (a) Lim, B. S.; Donahue, J.; Holm, R. H. *Inorg. Chem.* **2000**, *39*, 263. (b) Kapre, R. R.; Bothe, E.; Weyhermüller, T.; DeBeer George, S.; Wieghardt, K. *Inorg. Chem.* **2007**, *46*, 5642.

(19) (a) Stiefel, E. I.; Eisenberg, R.; Rosenberg, R. C.; Gray, H. B. *J. Am. Chem. Soc.* **1966**, *88*, 2956. (b) Sproules, S.; Bedito, F. L.; Bill, E.; Weyhermüller, T.; DeBeer George, S.; Wieghardt, K. *Inorg. Chem.* **2009**, *48*, 10926 and references therein.

(20) Campbell, S.; Harris, S. *Inorg. Chem.* **1996**, *35*, 3285.

(21) (a) Fourmigué, M.; Coulon, C. *Adv. Mater.* **1994**, *6*, 948. (b) Domercq, B.; Coulon, C.; Feneyrou, P.; Dentan, V.; Robin, P.; Fourmigué, M. *Adv. Funct. Mater.* **2002**, *12*, 359. (c) Nomura, M.; Sasaki, S.; Fujita-Takayama, C.; Hoshino, Y.; Kajitani, M. *J. Organomet. Chem.* **2006**, *691*, 3274. (d) Adams, H.; Gardner, H. C.; McRoy, R. A.; Morris, M. J.; Motley, J. C.; Torker, S. *Inorg. Chem.* **2006**, *45*, 10967.

(22) Inscore, F. E.; Knottenbelt, S. Z.; Rubie, N. D.; Joshi, H. K.; Kirk, M. L.; Enemark, J. H. *Inorg. Chem.* **2006**, *45*, 967.

Table 1. TBEs and TBE–so's (in brackets; eV) for the $[M(\text{dddt})_3]^{q-}$ and $[U(\text{dddt})_3(\text{py})]^{q-}$ Complexes ($M = \text{Nd}, \text{U}$)

complex	$[\text{Nd}(\text{dddt})_3]^{3-}$	$[\text{U}(\text{dddt})_3]^{3-}$	$[\text{U}(\text{dddt})_3]^{2-}$	$[\text{U}(\text{dddt})_3(\text{py})]^{3-}$	$[\text{U}(\text{dddt})_3(\text{py})]^{2-}$
spin state	quartet	quartet	triplet	quartet	triplet
isolated	–200.555 [–201.938]	–201.812 [–204.026]	–205.246 [–207.036]	–272.563 [–274.979]	–276.063 [–278.422]
THF solvated	–211.709	–213.313 [–215.625]	–211.921 [–213.715]	–283.856 [–286.384]	–281.853 [–284.244]
pyridine solvated	–212.401	–214.040 [–216.332]	–212.286 [–214.083]	–284.603 [–287.146]	–282.763 [–285.062]

complexes of a variety of metals²³ have been shown to exhibit strong folding effects,²⁴ which modulates the redox potential of the metal center by varying the $M-S$ covalency and leads to a stabilization of the most oxidized species through a similar second-order Jahn–Teller effect.²⁵ In these transition metal complexes, the possible involvement of a direct $M \cdots (C=C)$ interaction was evoked,²⁶ but in most cases, however, the smaller folding angles lead to $M \cdots (C=C)$ distances too long to authorize such conclusions. On the other hand, in the much strongly folded mono- and bis(dithiolene) organometallic derivatives of uranium,^{10,15} a direct $M \cdots (C=C)$ interaction has been unambiguously identified. The question then arises of whether a similarly strong $M \cdots (C=C)$ interaction is responsible for the very large folding angle of the MS_2C_2 moiety in the $M(\text{dddt})_3$ units of both Nd(III) and U(IV). Does such an interaction exist in the hypothetical U(III) counterpart, and is this complex predictably stable? Could such an interaction have a role in lanthanide(III)/actinide(III) differentiation? Relativistic DFT, which has shown its capacity to compute ground state properties of f element complexes with satisfying accuracy, should be appropriate to address these questions.^{2,16} Solvent effects (in that case, THF or pyridine) will be taken into account using the CONductor-like Screening Model (COSMO) for a realistic solvation approach.

Results and Discussion

Molecular Geometry Optimization. The molecular geometries of the tris(dithiolene) complexes $[M(\text{dddt})_3]^{q-}$ ($q=3, M = \text{Nd}^{3+}$ and $q=3, 2, M = \text{U}^{3+/4+}$) and $[M(\text{dddt})_3(\text{py})]^{3-}$ ($M = \text{Nd}^{3+}, \text{U}^{3+}$) have been fully optimized at the ZORA/DFT–BP86/TZP level, considering their highest spin states, utilizing the ADF package. Calculations were performed first on isolated species, starting from X-ray data when available, then in solution (THF and pyridine) using COSMO for a realistic solvation model (see Computational Details).

We discuss first the stabilities of the considered species on the basis of their Total Binding Energies (TBE) and their TBE including spin–orbit corrections (TBE–so). The latter corrections have been computed via a single point calculation using the previously optimized geometries. In Table 1 are given the computed values for the $[M(\text{dddt})_3]^{q-}$ and $[U(\text{dddt})_3(\text{py})]^{q-}$ complexes.

Considering the $[U(\text{dddt})_3]^{q-}$ uranium complexes, it can be seen that spin–orbit corrections lead to a non-negligible energy lowering of 2.2–2.3 eV for the U(III)

species in their quartet state and 1.8 eV for the U(IV) ones in their triplet state. We note also that this energy correction is almost the same in the gas phase as in solution, as expected because this correction is mainly of an atomic nature (see Computational Details), i.e., depending essentially on the uranium atom oxidation state and not on the molecular environment. Moreover, the greater stabilizing effect of spin–orbit coupling for the U(III) species relative to the U(IV) ones already appears considering the U(III) and U(IV) isolated ions, the computations of the spin–orbit energy corrections using ZORA/BP86/TZP calculations leading respectively to ca. 3.2 and 2.8 eV.

We have not been able to obtain converged results for the calculations including spin–orbit correction for the $[\text{Nd}(\text{dddt})_3]^{3-}$ species in solution. However, it is expected that the spin–orbit corrections to the energy of the latter complex, which have been computed for the isolated molecule, should be the same in solution, i.e., on the order of 1.4 eV.

It is worth noting that the U(IV) complex is more stable than the U(III) one in the gas phase, but less stable in solution. In order to investigate the question of the stability of the U(III) complex, we carried out the computation of the frequencies of its normal modes of vibration in the gas phase and in solution. It appears that the isolated as well as the solvated $[U(\text{dddt})_3]^{3-}$ U(III) species exhibit real vibrational frequencies (see the Supporting Information), indicating that the optimized structure corresponds to a minimum on the potential energy surface. The values in Table 1 show that the U(III) species is stabilized by a polar solvent relative to the U(IV) complex. The greater stabilization of the U(III) species relative to the U(IV) one in a polar solvent is mainly due to the highest charge borne by the former anion, –3 versus –2. Considering a more polar solvent than THF or py, like DMSO, its TBE reaches the value –214.888 eV, the vibration analysis indicating a thermodynamically stable structure in this solvent. However, our attempts to synthesize dithiolene complexes of uranium(III) were unsuccessful; treatment of $\text{U}(\text{I}_3)(\text{THF})_4$ or $\text{U}(\text{BH}_4)_3(\text{THF})_3$ with Na_2dddt invariably gave the U(IV) dithiolene complexes as the only identified products, whereas these latter, in the presence of reducing agents, were transformed into unidentified products. It is likely that the U(III) dithiolene complexes, if formed, undergo uncontrolled oxidation reactions, as previously observed with the U(III) thiolate compounds $\text{U}(\text{SMes}^*)_3$ ($\text{Mes}^* = 2,4,6\text{-}t\text{-Bu}_3\text{C}_6\text{H}_2$).²⁷

Looking now at the optimized geometries (Figure 2), it should be recalled that the sole tris(dithiolene) uranium complex which has been crystallographically characterized is the mononuclear U(IV) ion $[U(\text{dddt})_3]^{2-}$, and that

(23) (a) Fourmigué, M. *Coord. Chem. Rev.* **1998**, *180*, 823. (b) Cranswick, M. A.; Dawson, A.; Cooney, J. J. A.; Gruhn, N. E.; Lichtenberger, D. L.; Enemark, J. H. *Inorg. Chem.* **2007**, *46*, 10639.

(24) Lauher, J. W.; Hoffmann, R. *J. Am. Chem. Soc.* **1976**, *98*, 1729.

(25) Fourmigué, M. *Acc. Chem. Res.* **2004**, *37*, 179.

(26) Moriarty, R. E.; Ernst, R. D.; Bau, R. *J. Chem. Soc., Chem. Commun.* **1972**, 1242.

(27) Roger, M.; Barros, N.; Arliguie, T.; Thuéry, P.; Maron, L.; Ephrikhine, M. *J. Am. Chem. Soc.* **2006**, *128*, 8790.

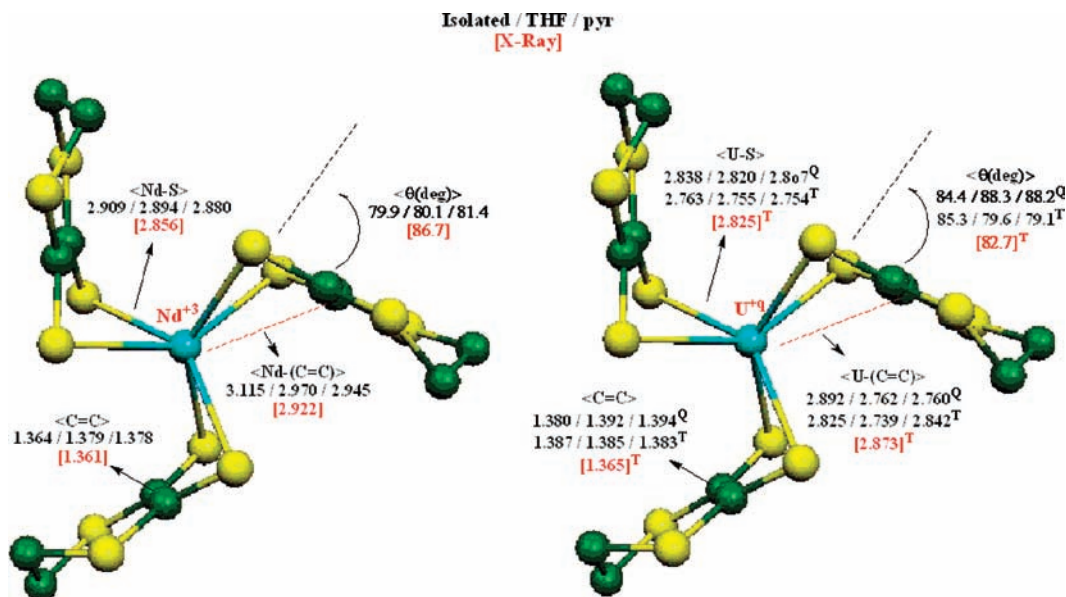


Figure 2. Optimized geometries, calculated and experimental (in brackets) mean bond distances (Å) and angles (deg) of the Nd^{3+} and $\text{U}^{+3,+4}$ $\text{M}(\text{dddt})_3$ species (Q indicates U(III) values and T, U(IV) ones). H atoms omitted for clarity.

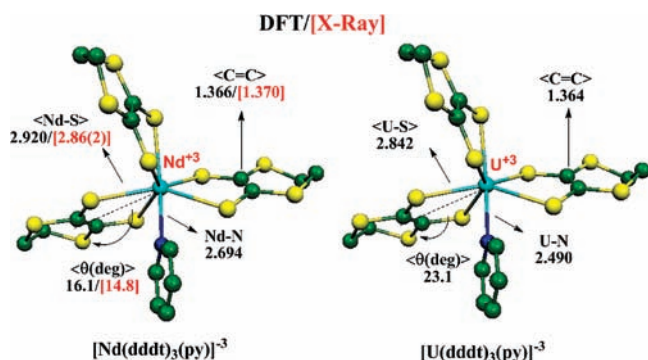


Figure 3. Optimized geometries, calculated and experimental (in brackets) mean bond distances (Å) and angles (deg) of $[\text{Nd}(\text{dddtd})_3(\text{py})]^{3-}$ and $[\text{U}(\text{dddtd})_3(\text{py})]^{3-}$. H atoms omitted for clarity.

the Nd(III) species $[\text{Nd}(\text{dddtd})_3]^{3-}$ was found in the $[\text{Na}_{1.5}\text{Nd}(\text{dddtd})_3]^{1.5-}$ polymer (Figure 1).

The computed geometries of the two mononuclear Nd(III) and U(III) tris(dithiolene) complexes containing the pyridine ligand, i.e., $[\text{Nd}(\text{dddtd})_3(\text{py})]^{3-}$, which was isolated,^{13a} and $[\text{U}(\text{dddtd})_3(\text{py})]^{3-}$ are displayed in Figure 3. These complexes do not exhibit any significant folding of the dddtd ligands.

Relevant metal–ligand distances and bond angles with the corresponding experimental data are reported in Table 2. The M–S, S–C, and $\text{M}\cdots(\text{C}=\text{C})$ distances are averaged over the three dddtd ligands of each species. The $\text{M}\cdots(\text{C}=\text{C})$ distance is measured between the metal center and the middle of the C=C bond. Average M–C distances, C=C bond lengths, and the dihedral folding angles θ of the MS_2C_2 metallacycle are also given for comparison with X-ray data.

The optimized geometries of the Nd(III) and U(IV) complexes $[\text{Nd}(\text{dddtd})_3(\text{py})]^{3-}$ and $[\text{U}(\text{dddtd})_3]^{2-}$ are in very good agreement with the experimental ones, with deviations in bond lengths and angles not exceeding 0.06 Å and 2°. The calculations reproduce nicely the folding angle of the MS_2C_2 metallacycle. The maximum deviations are slightly larger

between the calculated distances and angles of $[\text{Nd}(\text{dddtd})_3]^{3-}$ and the values measured in the crystal structure of the polymer $[\text{Na}_{1.5}\text{Nd}(\text{dddtd})_3]^{1.5-}$; in particular, the folding angle of the dddtd ligand θ is 7° larger in the polymer, likely reflecting the presence of steric effects. Expectedly, the shortening of the U–S and U–C distances passing from U^{3+} to U^{4+} is consistent with the ionic radii variation.²⁸

The computed Nd(III) and U(III) complexes exhibit a similar molecular structure (Figures 2 and 3) but present some significant geometrical differences. The average M–S distance is 0.07 Å shorter for $\text{M} = \text{U}$ than for $\text{M} = \text{Nd}$, whereas the ionic radius of Nd(III) is 0.04 Å smaller than that of U(III).²⁸ This difference reflects the more covalent character of the M–S bonding in the actinide compound. The variation in the computed θ angles of the $[\text{M}(\text{dddtd})_3]^{q-}$ species reveals that the folding of the dddtd ligand increases when passing from the Nd(III) to the U(III) complexes (i.e., 79.9 vs 84.4°) and from the U(III) to U(IV) species. Alternatively, the computed $\text{M}\cdots(\text{C}=\text{C})$ distances are 3.115 Å for the Nd(III) complex vs 2.892 and 2.825 Å on average for the U(III) and U(IV) species, while the computed C=C distance increases from Nd(III) (1.364 Å) to the U(III) and U(IV) complexes (1.380 and 1.387 Å). This trend is in accordance with the experimental values for the Nd(III) and U(IV) complexes. It thus appears that during the oxidation process of the uranium species $[\text{U}(\text{dddtd})_3]^{q-}$ ($q = 3, 2$) the C=C double bond gets longer with the metal center coming closer to this double bond. These structural features strongly suggest the occurrence of an attractive interaction between uranium and the dithiolene C=C double bond. This question will be investigated in more detail hereafter. As it has been said above, the $[\text{M}(\text{dddtd})_3(\text{py})]^{3-}$ complexes exhibit practically no folding of the Mdddtd metallacycle; indeed the presence of the pyridine ligand prevents such folding for steric and electronic reasons.

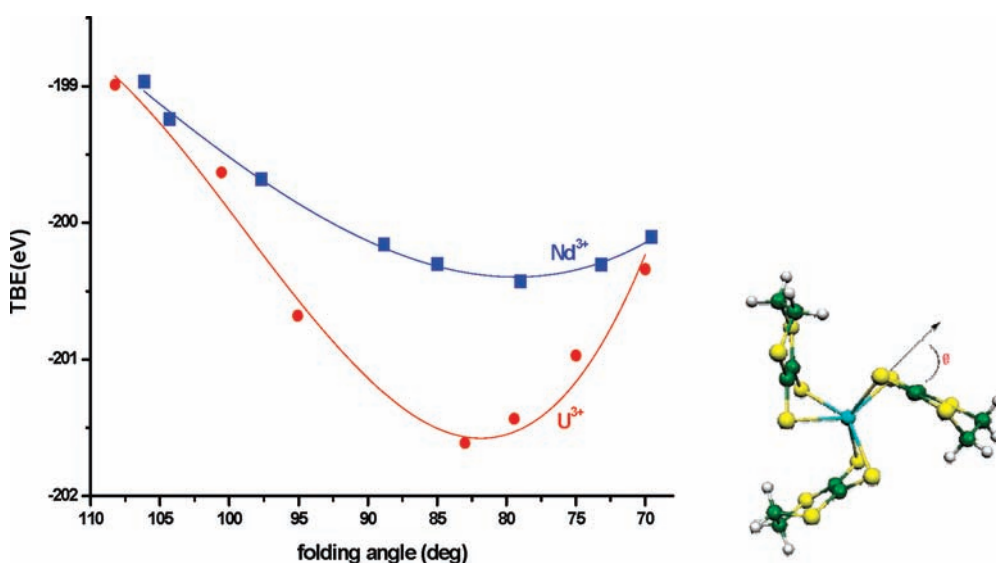
Considering now the S–C bond lengths given in Table 2, it can be seen that their values, which compare

(28) Shannon, R. D. *Acta Crystallogr., Sect. A* 1976, 32, 751.

Table 2. Relevant Bond Distances (Å) and Angles θ (deg) of $[M(\text{dddt})_3(\text{py})]^{3-}$ and $[M(\text{dddt})_3]^{q-}$ Species ($M = \text{Nd}^{3+}, \text{U}^{3+/4+}; q = 3, 2$) with Available X-Ray Data (in Square Brackets)

spin state	$[M(\text{dddt})_3]^{q-}$			$[M(\text{dddt})_3(\text{py})]^{3-}$	
	Nd^{3+}	U^{3+}	U^{4+}	Nd^{3+}	U^{3+}
	quartet	quartet	triplet	quartet	quartet
M–S	2.895–2.926 <2.909> [2.829–2.882] ^a [<2.86(2)>]	2.820–2.860 <2.838>	2.727–2.779 <2.763> [2.717–2.760] [<2.737(14)>]	2.874–2.936 <2.920> [2.817–2.872] [<2.86(2)>]	2.818–2.853 <2.842>
M···(C=C)	3.091–3.148 <3.115>	2.856–2.941 <2.892>	2.766–2.862 <2.825>		
M–C	<3.190>	<2.870>	<2.912>		
S–C	[<2.92(2)>] ^a 1.756–1.815 <1.779> [<1.766>]	1.757–1.764 <1.760>	[<2.87(3)>] 1.753–1.762 <1.756> [<1.768(2)>]	1.751–1.760 <1.758> [<1.76(3)>]	1.756–1.770 <1.760>
C=C	<1.364> [<1.361>] ^a	<1.380>	<1.387> [<1.365(9)>]	<1.366> [<1.355(7)>]	<1.364>
θ	<79.9> [<86.7>] ^a	<84.4>	<85.3> [<82.7>]	<16.1> [<14.8>]	<23.1>

^a X-ray data of the Nd(III) polymeric species.

**Figure 4.** Energy variation vs folding angle in the complexes $[M(\text{dddt})_3]^{3-}$ ($M = \text{Nd}, \text{U}$).

very well with the available X-ray data, depend very slightly on the nature of the metal or its oxidation state. Moreover, the average S–C distances of 1.766 and 1.768 Å for Nd(III) and U(III) species, respectively, and 1.76(3) Å for $[\text{Nd}(\text{dddt})_3(\text{py})]^{3-}$ are similar to those found in $[\text{Mo}(\text{Cp})_2(\text{dddt})]$, 1.76(1) Å.^{15c} These results suggest that the redox active dddt ligands are rather “innocent” in these complexes.

The main investigated issue of this study is the origin of the folding angle of the Mdddt metallacycle; this group is quite flexible,²⁹ but the reason for its large folding in the $[M(\text{dddt})_3]^{q-}$ complexes under consideration is questionable. In Figure 4 are shown the variations of the energy of the complexes $[M(\text{dddt})_3]^{3-}$ ($M = \text{Nd}, \text{U}$) as a function of the folding angle θ . These curves have been plotted step by step following Linear Transit (LT) calculations, the

atomic coordinates being allowed to relax at all points for every fixed value of the folding angle.

As it can be seen, the potential well is deeper for the U(III) complex; the Mdddt metallacycle of the Nd(III) complex is allowed to be more flexible, within a large range of angles around the energy minimum, contrarily to the U(III) complex. Furthermore, it is worth noting that the vibration analysis shows that the computed equilibrium structure of the Nd(III) species exhibits two imaginary frequencies (computed analytically) at $i12 \text{ cm}^{-1}$ and $i4 \text{ cm}^{-1}$, the former corresponding to a reduction of the folding angle θ . We remind that all vibration frequencies of the U(III) complex are real. The discussion of these crucial differences between the two species will be detailed later in the text.

In Table 3 are listed the computed geometrical parameters of the $[M(\text{dddt})_3]^{3-}$ ($M = \text{Nd}, \text{U}$) and $[\text{U}(\text{dddt})_3]^{2-}$ complexes in the gas phase and in solution (THF, pyridine). The optimized structures are given in the Supporting Information. From these data, it appears that a polar solvent induces a shortening of the M–S and M···(C=C)

(29) (a) Arliguie, T.; Thuéry, P.; Fourmigué, M.; Ephritikhine, M. *Organometallics* **2003**, *22*, 3000. (b) Arliguie, T.; Thuéry, P.; Fourmigué, M.; Ephritikhine, M. *Eur. J. Inorg. Chem.* **2004**, 4502.

distances of the U(III) and Nd(III) complexes, this shortening increasing with the solvent polarity. Concomitantly, the dddt folding angle in these complexes increases, especially in $[\text{U}(\text{dddt})_3]^{3-}$, and the C=C bond lengths increase in both species.

Concerning the geometry of the U(IV) complex, contrarily to the U(III) and Nd(III) species, a lengthening of the $\text{M}\cdots(\text{C}=\text{C})$ distance and a decrease of the folding angle for this complex can be noted in solution. In a parallel way, the C=C distance shortens. However, these effects remain less important than in the trianionic species.

These geometrical differences between the U(III) and U(IV) complexes, which are consistent with the aforementioned greater stabilization of the U(III) species in a polar solvent, bring to light the importance of the $\text{M}\cdots(\text{C}=\text{C})$ interaction under consideration, which will be confirmed by the electronic structure analysis given below.

Table 3. Solvent Effects on Geometries^a

	$[\text{Nd}(\text{dddt})_3]^{3-}$ Nd(III)	$[\text{U}(\text{dddt})_3]^{3-}$ U(III)	$[\text{U}(\text{dddt})_3]^{2-}$ U(IV)
<M–S>	2.909/2.894/ 2.880	2.838/2.820/ 2.807	2.763/2.755/ 2.754
<M⋯ (C=C)>	3.115/2.970/ 2.945	2.892/2.762/ 2.760	2.825/2.839/ 2.842
<M–C>	3.190/3.040/ 3.031	2.870/2.830/ 2.827	2.912/2.920/ 2.931
<C=C>	1.364/1.378/ 1.379	1.380/1.392/ 1.394	1.387/1.385/ 1.383
<θ>	79.9/80.1/ 81.4	84.4/88.3/ 88.2	85.3/79.6/ 79.1

^a Average distances (Å) and angles (deg) calculated in the gas phase/THF/pyridine.

Molecular Orbital (MO) Analysis. MO diagrams of the trivalent neodymium (left) and uranium (middle) $[\text{M}(\text{dddt})_3]^{3-}$ complexes in their quartet state and the uranium(IV) $[\text{U}(\text{dddt})_3]^{2-}$ derivative (right) in its triplet state are displayed in Figure 5. The percentages (d/f/M) represent respectively the d and f metal orbital contributions to the MOs and the total metallic weight. For the frontier singly occupied MOs (SOMOs), (d/f/M/ligand) weights are given.

These diagrams show that there are two important sets of frontier MOs for the Nd(III) and U(III) systems. The highest occupied α spin-orbitals, i.e., SOMO, SOMO–1, and SOMO–2 (MO #76, 75, and 74) are quite different in the two complexes.

In $[\text{Nd}(\text{dddt})_3]^{3-}$, these MOs appear to be essentially metallic, with a strong 4f orbital character and zero contribution from the dithiolene ligands as indicated by the percentage % (d/f/Nd/ligand). The 4f block is deep in energy, confirming its slight participation in the metal–ligand bonding. The MOs immediately below are slightly different in energy, and their orbital composition shows that the 5d and 4f orbital weights remain small.

On the contrary, in the U(III) system, the two highest singly occupied MOs, namely, the SOMO–1 and SOMO–2 (MO #75 and 74) are delocalized over the metal and the ligands as indicated by the percentage % (d/f/U/ligand). The U/ligand orbital mixings (i.e., 71/14 and 70/15% for MO #75 and 74, respectively) reveal the significant metal-to-ligand back-donation. The shape of SOMO–1 et SOMO–2 indicates the occurrence of a charge transfer between the central U(III) atom and the C=C double bond of each dithiolene ligand. This charge transfer is ensured by a significant contribution of the

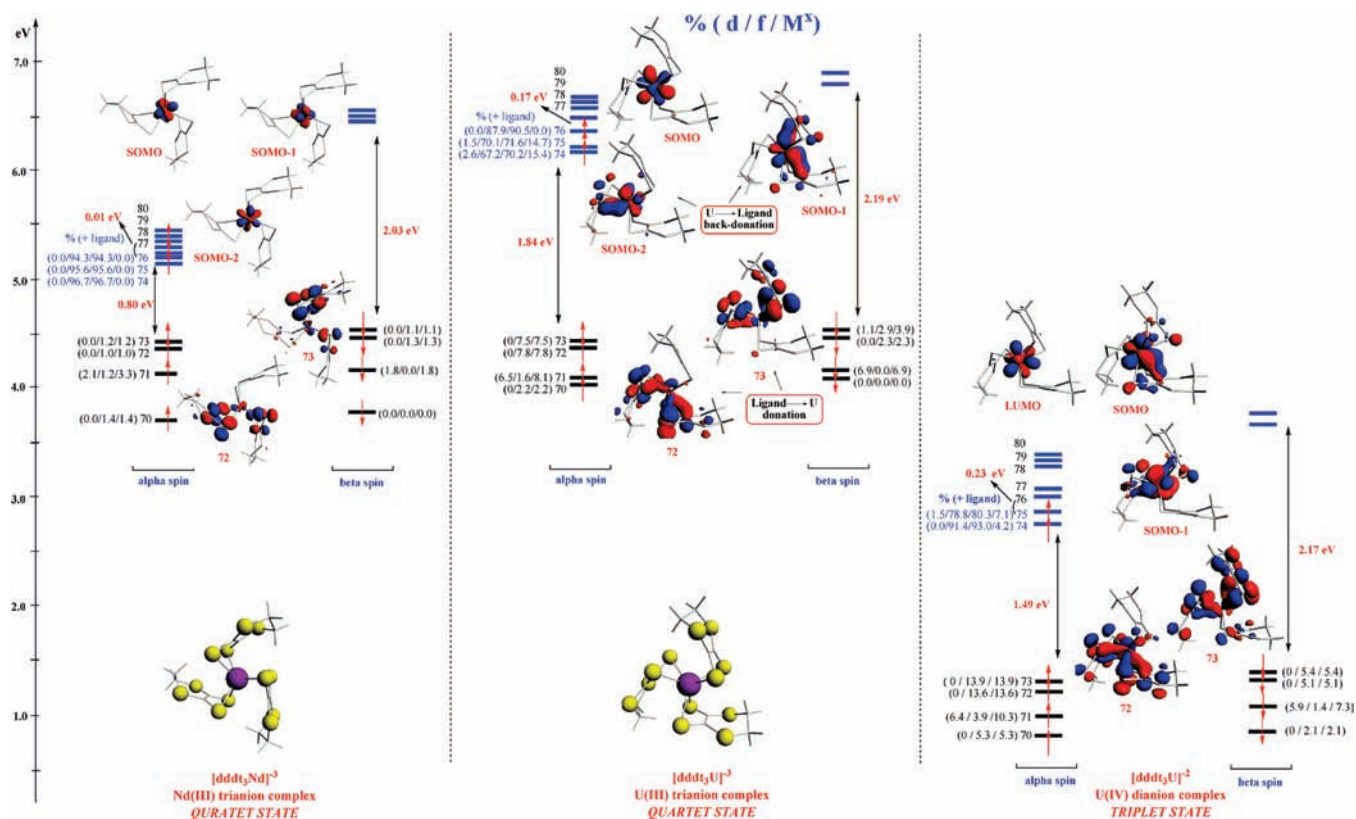


Figure 5. Frontier MO diagrams of Nd(III) and U(III) $[\text{M}(\text{dddt})_3]^{3-}$ and U(IV) $[\text{U}(\text{dddt})_3]^{2-}$ complexes.

Table 4. $\%(d/f/M)$ α Spin–Orbital Composition of $M(\text{dddt})_3^{q-}$ ($M = \text{Nd}^{3+}$, U^{3+} , and U^{4+})

% (d/f/M)	Nd(III)		U(III)		U(IV)	
	isolated	solvated ^a	isolated	solvated ^a	isolated	solvated ^a
SOMO 76	(0/94.3/94.3/0)	(0/93.2/93.2/0)	(0/87.9/90.5/0)	(0/88.6/90.8/0)		
75	(0/95.6/95.6/0)	(0/94.4/94.4/0)	(1.5/70.1/71.6/14.7)	(1.7/71.9/73.6/18.1)	(1.5/78.8/80.3/7.1)	(0/83.3/83.3/4.8)
74	(0/96.7/96.7/0)	(0/98.1/98.1/0)	(2.6/67.2/70.2/15.4)	(3/68.6/71.6/17.2)	(0/91.4/93.0/4.2)	(0/92/93.6/2.0)
73	(0/1.2/1.2)	(0/3.8/3.8)	(0/7.5/7.5)	(0/8.7/8.7)	(0/13.9/13.9)	(0/10.1/10.1)
72	(0/1.0/1.0)	(0/1.7/1.7)	(0/7.8/7.8)	(1.2/9.1/9.1)	(0/13.6/13.6)	(0/11.5/11.5)

^a Solvent = pyridine.

uranium 5f orbitals taking part in a $\text{U(III)} \cdots (\text{C}=\text{C})$ interaction, as suggested by the structural features. The ligand-to-metal donation present in the U(III) complex is well described by MOs #73 and 72 below SOMO–2, as shown by the percentage composition $\%(d/f/U)$. The $\text{C}=\text{C}$ double bond donation toward the uranium ion is particularly noticeable. Finally, the U(III) complex exhibits a more important covalent character of bonding than in the Nd(III) species.

Considering the latter MOs #73 and 72 of the U(IV) species, it can be seen that the ligand to metal donation, as indicated by the metal contribution to these MOs, is higher than in the U(III) complex. This confirms the ability of the dithiolene ligand to stabilize uranium high oxidation states ($> +3$). On the contrary, the metal orbitals' weights in SOMOs #74 and 75 are higher for the U(III) than for the U(IV) complex, indicating a more important metal-to-ligand back-donation, namely to the $\text{C}=\text{C} \pi^*$ MO, in the trianionic species. This difference between the bonding MOs of the U(III) and U(IV) complexes can be understood considering the relative energies of the metal and ligand orbitals. Indeed, the higher oxidation state of the U(IV) species lowers the metal AO energies, bringing them into closer match with the filled ligand levels, so explaining the more significant ligand-to-metal donation. The lower oxidation state of U(III) makes metal AOs closer to $\text{C}=\text{C} \pi^*$ reinforcing the metal-to-ligand back-donation.

The splitting of the 5f orbitals block relative to the 4f one gives more evidence for their participation in metal–ligand bonding. Indeed, for the U(III) and U(IV) complexes, the SOMO–LUMO gaps (Figure 5) reach 0.17 and 0.23 eV, respectively. For the Nd(III) complex, the same splitting reaches only a value of 0.01 eV for the 4f manifold, thus indicating that the latter orbitals are practically not involved in metal to ligand bonding. This splitting is found to be significant only in the actinide systems; it is indicative of the stabilization of the molecular entities due to the participation in bonding of the 5f uranium orbitals.

In Table 4 is reported the MO composition analysis in terms of $\%(d/f/M)$ of the SOMO levels with % ligands (i. e., MO #76, 75 and 74) for the isolated and solvated (pyridine) trivalent $M(\text{dddt})_3^{3-}$ Nd(III) and U(III) species. These results highlight the more important effect of the pyridine solvent on the U(III) species by comparison with the Nd(III) analogue.

The retro-donation related to the $\text{U(III)} \cdots (\text{C}=\text{C})$ interaction is reinforced in the solvent, the ligand contribution being augmented significantly; we note also the increase of the U(III) 5f orbital weights in SOMO–1 and SOMO–2.

In the U(IV) SOMOs #75 and 74, the contribution of 5f orbitals is larger, but that of ligands is smaller. The weight of the metal orbitals in MOs #73 and 72 decreases in the presence of the solvent. These two facts agree well with the lengthening of the $\text{U} \cdots (\text{C}=\text{C})$ distances in the solvated U(IV) complex. This also corroborates, as mentioned, the fact that the U(III) species is more stabilized by a polar solvent. This stabilization is partly due to electronic effects which enhance the ligand-to-metal donation and metal-to-ligand retro-donation related to the $\text{U(III)} \cdots (\text{C}=\text{C})$ interaction.

The electron population analyses which are developed below give further arguments, permitting a better understanding of the difference between the Nd(III) and U(III) complexes and of the origin of the Mdddt folding in these species.

Population Analyses. A Mulliken population analysis (MPA) was first carried out. Despite its known drawbacks, MPA remains a useful tool to compare the variation of electronic populations in homologous series of compounds computed at the same level of theory. In Table 5 are given the computed MPA net charges q_M and q_S ; the metallic spin densities ρ_M equal the difference between the total α and β electronic populations of the metal, and overlap populations. We remind that for all systems (see the Computational Details), the trianionic f^3 complexes are considered in their quartet (Q) state, i. e., $\text{Nd(III)} 4\text{f}^3$ and $\text{U(III)} 5\text{f}^3$ configurations. The dianionic $\text{U(IV)} 5\text{f}^2$ system is considered in its triplet (T) spin state.

In all complexes, the metallic net charges q_M are significantly smaller than the ion formal oxidation states, although MPA generally overestimates this fact. This trend is a clear indication of the important electronic charge transfer from the dithiolene ligands toward the central metal, as already noted in other uranium dithiolene species.^{10b} The donation effect of the pyridine ligand, in the $[\text{M}(\text{dddt})_3(\text{py})]^{q-}$ complexes, leads to a further reduction of the metallic net charge. The net charges of Nd(III) remain significantly larger than the U(III) ones, indicating a smaller ligand-to-metal donation in the former. Alternatively, the calculated negative charges of the adjacent sulfur atoms are slightly smaller for U(III) than for Nd(III) (–0.29 vs –0.33). Finally, the MPA metallic spin density is much larger for Nd(III) than for U(III) (3.30 vs 2.70), giving another evidence of the larger back-donation from the uranium(III) metal center to the dithiolene ligand.

The larger $\text{M}–\text{S}$ overlap population in the U(III) species confirms the more covalent character of this bond by comparison with the Nd(III) congener. The calculations reveal the significant $\text{U} \cdots (\text{C}=\text{C})$ overlap population and sustain the occurrence of a covalent attractive

Table 5. MPA Spin Densities, Net Charges, and Atom–Atom Overlap Populations

structure	M^{q+}	spin state	MPA			overlap populations		
			ρ_M	q_M	$\langle q_S \rangle$	M–S	$M \cdots (C=C)$	(C=C)
$[\text{Nd}(\text{ddd}t)_3]^{3-}$	Nd^{3+}	Q	3.30	+1.11	–0.33	0.147	–0.028	0.525
$[\text{U}(\text{ddd}t)_3]^{3-}$	U^{3+}	Q	2.70	+0.60	–0.29	0.166	0.013	0.355
	$x = 3$							
	$x = 2$							
$[\text{Nd}(\text{ddd}t)_3(\text{py})]^{3-}$	Nd^{3+}	T	2.18	+0.51	–0.20	0.168	0.018	0.346
$[\text{U}(\text{ddd}t)_3(\text{py})]^{3-}$	U^{3+}	Q	3.32	+0.86	–0.34			
		Q	2.61	+0.45	–0.22			

Table 6. Mayer Orbital–Orbital Populations and Atom–Atom Bond Orders

structure	spin state	atom–atom bond order				
		$\langle S(3p) \rangle$	$\langle C=C(2p) \rangle$	$\langle M-S \rangle$	$\langle M \cdots (C=C) \rangle$	$\langle C=C \rangle$
$[\text{Nd}(\text{ddd}t)_3]^{3-}$	quartet					
	d	0.082	0.000	0.756	0.008	1.457
	f	0.014	0.004			
$[\text{U}(\text{ddd}t)_3]^{3-}$	quartet					
	d	0.067	0.012	0.811	0.063	1.346
	f	0.113	0.020			
$[\text{U}(\text{ddd}t)_3]^{2-}$	triplet					
	d	0.071	0.014	0.870	0.087	1.337
	f	0.124	0.022			

interaction. That of $\text{Nd}(\text{III}) \cdots (\text{C}=\text{C})$ is negative and indicates a rather anti-bonding interaction. Moreover, the electronic population of the $\text{C}=\text{C}$ bond is significantly smaller in the uranium species, in relation with its elongation when it is close to the central metal, and confirms the donation and retrodonation transfers already brought to light by the MO analysis.

The results of the Mayer analysis give further insight into the electronic interactions driving the structure of the species under consideration.

The Mayer orbital–orbital populations and atom–atom bond orders are known to be reliable tools to get insight into the metal–ligand bonding and to investigate the role of the d and f orbitals.^{19,30} The values of the Mayer bond order resemble classical atom–atom bond multiplicities, i.e., roughly equal to 1, 2, or 3 for a single, double, or triple bond, respectively. However, this bond order depends on the used basis set, so that comparisons between different systems are valid only if analogous basis sets are used, but it is worth noting that this index only slightly depends on the used DFT functional. The Mayer atom–atom bond order between two atoms is given as the sum over pairs of atomic orbitals, one of each atom.

In Table 6 are given the d and f contributions to the $\text{M}-\text{S}(3p)$ and $\text{M} \cdots \text{C}=\text{C}(2p)$ interactions. Once again, we note that the orbital–orbital population is more important between 5f orbitals and the sulfur 3p electron lone pairs for the uranium species, with a significant contribution of the 6d orbitals. On the contrary, in the neodymium complex, the 5d orbitals dominate the $\text{M}-\text{S}$ bonding with a negligible contribution of the 4f orbitals. The bond order correlates with this feature with more covalent and stronger $\text{U}-\text{S}$ bonds. Considering the $\text{M} \cdots (\text{C}=\text{C})$ interaction, it can be seen that the 5f orbital contribution, although small, is larger than that of the 6d

Table 7. Solvent Effect on MPA Overlap Populations

structure gas/ THF/py	$[\text{Nd}^{\text{III}}(\text{ddd}t)_3]^{3-}$	$[\text{U}^{\text{III}}(\text{ddd}t)_3]^{3-}$	$[\text{U}^{\text{IV}}(\text{ddd}t)_3]^{2-}$
$\langle \text{M}-\text{S} \rangle$	0.147/0.150/ 0.159	0.166/0.176/ 0.188	0.168/0.177/ 0.179
$\langle \text{M} \cdots$ $(\text{C}=\text{C}) \rangle$	–0.028/–0.029/ –0.031	0.013/0.016/ 0.017	0.018/0.015/ 0.014
$\langle (\text{C}=\text{C}) \rangle$	0.525/0.430/ 0.427	0.355/0.320/ 0.318	0.346/0.360/ 0.368

orbitals, thus confirming their role in such an interaction. In the same way, the $\text{M} \cdots (\text{C}=\text{C})$ bond order is significantly large and accompanied by the weakening of the $\text{C}=\text{C}$ double bonds in the uranium species, whereas the $\text{Nd} \cdots (\text{C}=\text{C})$ bond order is very small and the $\text{C}=\text{C}$ bond order is high in the neodymium counterpart.

We found it interesting to investigate the solvent effect on the electronic population. The MPA results are shown in Table 7.

In the $\text{U}(\text{III})$ complexes, the significant increase of the $\text{U} \cdots (\text{C}=\text{C})$ population and the reduction of the population of the $\text{C}=\text{C}$ bond with solvation is related to the higher ligand-to-metal donation and metal-to-ligand retrodonation. On the contrary, as expected, these populations, especially the $\text{C}=\text{C}$ one, vary in an opposite direction in the $\text{U}(\text{IV})$ complex.

Conclusion

The structures of the homoleptic lanthanide and actinide tris(dithiolene) complexes have been studied with the use of relativistic DFT, including spin–orbit corrections, solvent effects being taken into account using the COSMO model. This investigation has shown that the very large folding of the dithiolene ligands exhibited in uranium complexes $[\text{U}(\text{ddd}t)_3]^{3-}$ may be attributed to the occurrence of $\text{U} \cdots (\text{C}=\text{C})$ interactions between the central metal and the dithiolene ligands. A polar solvent reinforces this interaction in the $\text{U}(\text{III})$ case but weakens it in the $\text{U}(\text{IV})$ one, whereas no such interaction appears in the case of the $\text{Nd}(\text{III})$ complex, the overcrowding in the polymeric structure of this species

(30) (a) Mayer, I. *Chem. Phys. Lett.* **1983**, *97*, 270. Addendum **1985**, *117*, 396. (b) Mayer, I. *J. Comput. Chem.* **2007**, *28*, 204. (c) Bridgeman, A. J.; Cavigliasso, G.; Ireland, L. R.; Rothery, J. J. *Chem. Soc., Dalton Trans.* **2001**, 2095.

enforcing the folding of the metallacycle. Related to Ln(III)/An(III) differentiation, striking differences between the electronic structures of the Nd(III) and U(III) complexes appear also when comparing their frontier MOs, namely the important contribution to bonding of the 5f uranium orbitals relative to the 4f neodymium ones with a noticeable back-donation from the uranium metal to the ligands. Although the [U(ddd)₃]³⁻ complex has not yet been isolated, this study brings to light its greater thermodynamic stability with respect to the U(IV) and Nd(III) congeners, by emphasizing the major role that could be played by the metal···(C=C) interactions in lanthanide(III)/actinide(III) differentiation.

Computational Details

The calculations were performed using DFT with relativistic corrections being introduced via the Zero-Order Regular Approximation (ZORA).^{31,32} These ZORA/DFT calculations were performed using the Amsterdam Density Functional (ADF2007.01) program package.³³ The Vosko–Wilk–Nusair functional (VWN)³⁴ for the local density approximation (LDA) and the gradient corrections for exchange and correlation of Becke and Perdew,³⁵ respectively, i.e., the BP86 functional, have been used. Triple- ζ Slater-type valence orbitals (STO) augmented by one set of polarization functions were used for all atoms. Several studies have shown that such a ZORA/DFT/BP86/TZP approach reproduces the experimental geometries and ground state properties of f-element compounds with satisfying accuracy.^{11b–h}

For all elements, the basis sets were taken from the ADF/ZORA/TZP database. The frozen-core approximation where the core density is obtained from four-component Dirac–Slater calculations has been applied for all atoms. 1s core electrons were frozen respectively for carbon C[1s] and nitrogen N[1s]. For sulfur S[2p], the 1s/2s/2p core was frozen. The Nd[4d] and U[5d] valence space of the heavy elements includes the 4f/5s/5p/5d/6s/6p and 5f/6s/6p/6d/7s/7p shells (14 valence electrons), respectively.

For all complexes, we considered the highest spin state as the ground state; a single Slater determinant can be written for the highest spin state of an open-shell polyelectronic system, whereas several determinants are needed to describe a lower spin state of the same system.

The trianionic f³ complexes are considered in their quartet (Q) state, i.e., Nd(III) 4f³ and U(III) 5f³ configurations. The dianionic U(IV) 5f² system is considered in its triplet (T) spin

state. Because of SCF convergence problems, optimized geometries could only be obtained using the following procedure: we started the computations at the spin restricted level using first a DZP (STO double- ζ plus polarization) basis set, allowing electron smearing (high energy f electrons can be spread over several highest orbitals). Then, the smearq parameter which drives the electron smearing was progressively reduced. Then, using the DZP density as a restart, spin unrestricted TZP computations were carried out, reducing progressively the smearq parameter, until reaching the optimized geometries; so doing, an electronic aufbau configuration with no electron smearing was obtained for all species. Analytical vibration frequency calculations were then carried out, using an integration factor of 7, which should ensure good accuracy. It must be noted that a great number of cycles were often necessary to achieve SCF convergence especially for the M(III) species, owing to the quasi degeneracy of the highest occupied orbitals.

Next, the geometries were reoptimized in the solvent using the COSMO (Conductor-like Screening Model) for a realistic solvation approach.³⁶ We used the recommended non-default Delley type of cavity,^{36c} the solvent being considered with its dielectric constant (eps) of 7.58 and 11.75 for THF and pyridine, respectively. Finally, single point calculations including spin–orbit corrections were carried out using the previously optimized geometries, for both the gas phase and the solution. In general, in the case of closed shell molecules, it has been shown that spin–orbit coupling has important effects on energies but few effects on ground-state geometry and vibrational frequencies because of the quasiautomatic nature of this coupling.^{32c,37} Moreover, it is interesting to note that in the case of PtF₆ Arratia-Perez and co-workers³⁸ have found that ZORA two-component calculations including spin–orbit give the same tendency as the four-component DIRAC calculations.

Molecular geometries and molecular orbital plots were generated by using the MOLEKEL 4.3³⁹ and the ADF-VIEW³³ programs, respectively.

Acknowledgment. We thank the French and Algerian governments for a research grant: DPGRF/CNRS Project 2007–2009. Computing facilities were provided by IDRIS, CNRS Computing Center.

Supporting Information Available: Optimized coordinates and theoretical IR spectra. This material is available free of charge via the Internet at <http://pubs.acs.org>.

(31) (a) Baerends, E. J.; Ellis, D. E.; Ros, P. *J. Chem. Phys.* **1973**, *2*, 41. (b) Versluis, L.; Ziegler, T. *J. Chem. Phys.* **1988**, *88*, 322. (c) te Velde, G.; Baerends, E. J. *J. Comput. Phys.* **1992**, *99*, 84.

(32) (a) van Lenthe, E.; Baerends, E. J.; Snijders, J. G. *J. Chem. Phys.* **1993**, *99*, 4597. (b) van Lenthe, E.; Baerends, E. J.; Snijders, J. G. *J. Chem. Phys.* **1994**, *101*, 9783. (c) van Lenthe, E.; Snijders, J. G.; Baerends, E. J. *J. Chem. Phys.* **1996**, *105*, 6505. (d) Fonseca, G. C.; Snijders, J. G.; te Velde, G.; Baerends, E. J. *Theor. Chem. Acc.* **1998**, *391*. (e) van Lenthe, E.; Ehlers, A.; Baerends, E. J. *J. Chem. Phys.* **1999**, *110*, 8943. (f) te Velde, G.; Bickelhaupt, F. M.; Baerends, E. J.; Fonseca, G. C.; van Gisbergen, S. J. A.; Snijders, J. G.; Ziegler, T. *J. Comput. Chem.* **2001**, *22*, 931.

(33) ADF2007.01, SCM; Theoretical Chemistry, Vrije University: Amsterdam, The Netherlands. <http://www.scm.com> (accessed Feb 2010).

(34) Vosko, S. D.; Wilk, L.; Nusair, M. *Can. J. Chem.* **1990**, *58*, 1200.

(35) (a) Becke, A. D. *Phys. Rev. A* **1988**, *38*, 3098. (b) Perdew, J. P. *Phys. Rev. B* **1986**, *34*, 7406.

(36) (a) Klamt, A.; Schüürmann, G. *J. Chem. Soc. Perkin Trans. 2* **1993**, 799. (b) Klamt, A. *J. Phys. Chem.* **1995**, *99*, 2224. (c) Klamt, A.; Jones, V. *J. Chem. Phys.* **1996**, *105*, 9972. (d) Klamt, A.; Jonas, V.; T. Bürger, T.; Lohrenz, J. C. *J. Phys. Chem. A* **1998**, *102*, 5074. (e) Delley, B. *Mol. Simul.* **2006**, *32*, 117. (f) Klamt, A. *COSMO-RS From Quantum Chemistry to Fluid Phase Thermodynamics and Drug Design*; Elsevier: Amsterdam, 2005, ISBN 0–444–51994–7.

(37) (a) Xiao, H.; Li, J. *Chin. J. Struct. Chem* **2008**, *27*, 967. (b) García-Hernández, M.; Lauterbach, C.; Krüger, S.; Matveev, A.; Rösch, N. *J. Comput. Chem.* **2002**, *23*, 834.

(38) Alvarez-Thon, L.; David, J.; Arratia-Pérez, R.; Seppelt, K. *Phys. Rev. A* **2008**, *77*, 034502.

(39) Flükiger, P.; Lüthi, H. P.; Portmann, S.; Weber, J. *MOLEKEL4.3*; Swiss Center for Scientific Computing: Manno, Switzerland, 2000. <http://www.cscs.ch> (accessed Feb 2010).